Journal of Thermal Analysis and Calorimetry (2023) 148:5335–5346
https://doi.org/10.1007/s10973-023-12066-8

Nanoporous carbon doped with metal oxide microsphere as renewable flame retardant for integrating high flame retardancy and antibacterial properties of thermoplastic polymer composites

Nour F. Attia[1]

Received: 19 July 2022 / Accepted: 1 March 2023 / Published online: 24 March 2023

Abstract
Innovative, renewable and cost-effective porous composites were developed for integrating high fire safety and antibacterial properties for thermoplastic polymers. Sustainable porous carbon sheets were developed from plum stones as fruits-by-products via single carbonization step affording dual environmental and economic benefits. The as-developed porous carbon own specific surface area of 165 $m^2\ g^{-1}$ which is characteristic of mesoporous feature of an average mesopore size of 2.1 nm, in addition to naturally doped nitrogen species. The obtained porous carbons sheets were dispersed in different mass loadings in to polystyrene matrix-producing polymer composites. Interestingly, SnO_2 microsphere of an average size of 2 µm was synthesized on the surface of developed porous carbon sheets producing new porous composites. The new composites were elucidated using XRD, FT-IR and SEM–EDS. Then, the developed composites were dispersed in polystyrene. The mass loadings were altered and studied. The progress in fire safety, thermal stability and antibacterial properties for developed polymer composites was studied. The flame retardancy of the new composites was significantly improved achieving rate of burning of 20.5 mm min^{-1} compared to 46.5 mm min^{-1} for blank polymer. This superior flame retardancy was corroborated by recording LOI value of 24.5% compared to 18% for virgin polymer. This attained flame retardancy was ascribed to the synergistic effect between porous carbon sheets contained nitrogen and SnO_2 microsphere. The new composites afford promising inhibition for bacterial growth achieving clear antibacterial inhibition zone of 11 mm compared to zero for blank sample. The flame retardancy action was studied and elucidated.

Keywords Fruits-by-product · Flame retardants · Renewable porous carbon · SnO_2 microsphere · Polymer composites · Antibacterial

Introduction

Due to their unique properties and affordable price, synthetic thermoplastic polymers are utilized in a wide range of applications [1–4]. Due to its exceptional merits, including good chemical stability, superior mechanical properties, ease of processing, and low density, polystyrene (PS) is a well-liked member and has the potential to be used in electronic, packaging, vehicle, electrical, and appliance applications [5–7]. However, due to its low thermal stability and significant flammability risks, which allow for quick ignition and easier combustion when exposed to an ignition source, its safe use in a range of applications has been severely constrained [1, 8, 9]. On the other hand, the outbreak of pandemic (viruses) and bacterial growth on polymers surface restricted its use in hospital and medical applications. Therefore, a variety of flame retardants materials have been used and involved as additives to PS in order to overcome these challenges and expand the industrial applications of PS. These materials range from halogenated compounds which were later restricted due to toxicity issues to phosphorus and nitrogen-based compounds. Afterward, nanoparticles were utilized affording good flame retardancy and toxic gases suppression [5, 10–13]. Additionally, several 2D nanosheets were also reported for enhancing thermal stability and flame retardancy of PS [5]. On the other hand, Tin dioxide (SnO_2) has attracted much attentions as flame retardant fillers for

✉ Nour F. Attia
drnour2005@yahoo.com

[1] Gas Analysis and Fire Safety Laboratory, Chemistry Division, National Institute of Standards, 136, Giza 12211, Egypt

thermoplastic polymers due to its intrinsic catalytic properties during combustion process. Thus, trigger earlier formation of protective char layer on surface of polymer composite isolatingthe flaming zone from polymer pyrolysis zone and in turn restrict the heat and mass transfer [14–17]. Consequently, SnO_2 was reported as flame retardants fillers in different forms and shape and in synergistic with other flame-retardant materials to achieve good flame retardancy effect [4, 18, 19]. However, they prefer aggregating together during the processing of SnO_2 particles in thermoplastic polymers rather than uniform dispersion in polymer matrix. Therefore, this affords inferior catalytic performance and then poor flame retardancy to attained polymer composites [16]. Hence, to address this issue and enhance the dispersibility of SnO_2 in polymer matrix some materials were suggested to be used act as support to retard the aggregation process [16, 20]. Moreover, other trials were executed to overcome this problem, such as functionalization of tin on nanoporous silica [21] and incorporation with other flame-retardant compounds [22]. Recently, there has been a trend in recycling agricultural wastes to produce porous carbon for uses such as gas capture and energy gas separation and storage [23–26]. Moreover, recently, porous carbon sheets were developed from sugar beet leaves and exploited as green and sustainable flame retardant and toxic gases suppressants [9]. It is interesting to note that plum fruit is grown extensively over the world, with Egypt producing 14,775 tons of plums annually, ranking 43rd among all countries [27]. In light of environmental concerns, a significant amount of plum stones (PSs) were produced (~ 10 mass% of plum mass) as waste due to the enormous amount of stones that were produced. In our previous studies, several green flame retardants were developed for thermoplastic polymers and rubbers presenting a good flame retardants and suppressants for toxic gases [9, 23, 28, 29]. Hence, in this study, for the first time, PSs as fruits-by-products and waste were recycled and valorized to nanoporous carbon sheets via one pot step and used as flame retardant material for PS. Additionally, the developed porous carbon-derived PSs were decorated with SnO_2 microspheres and exploited as green flame-retardant material for PS polymer composites. This affords excellent flame retardancy effect and prohibiting the growth of bacteria on the surface of as-developed polymer composite. Therefore, PSs as fruits-by-products were grinded and carbonized under inert atmosphere yielding nanoporous carbon sheets of PSs (PPSs) and then dispersed alone in PS forming PS-PPSs composites. Furthermore, SnO_2 microsphere was synthesized on PPSs surface producing PPSs-SnO_2 composites and then uniformly dispersed in PS matrix yielding new polymer composites PS. The mass loadings of both PPSs and PPSs-SnO_2 were altered. The structure and surface area of PPSs were elucidated. Additionally, the structure and morphology of PPSs-SnO_2 composite were studied using XRD, FT-IR and SEM–EDS. Furthermore, the dispersion of PPSs-SnO_2 in PS matrix was evaluated. The flammability, thermal stability and antibacterial properties of PS-PPSs-SnO_2 were studied and enhanced. The flame retardancy mechanistic action was proposed.

Experimental

Materials

Polystyrene as thermoplastic polymer was obtained from LG Chem, Korea. Plum stones were collected after eating of plum fruit bought from local markets. Chloroform and stannous chloride dihydrate were supplied from Sigma-Aldrich Chemie GMBH, Germany. Deionized water (DI) was used synthesis of composites and washing.

Synthesis of renewable and sustainable nanoporous carbon sheets-derived plum stones

Firstly, the plum fruit was bought from the local market and plum fruit was eaten by author and the stones were collected. Then, washed well with DI water to remove any plum impurities and then dried for 7 days under sun. Afterward, the obtained PSs were grinded in to small pieces and then carbonized at 800 °C for 1 h under nitrogen gas flow with heating rate of 5 °C min^{-1}. Then, the obtained porous carbons sheets were washed with DI water and dried in oven. The as-developed porous carbon was denoted as PPSs as P refers to porous carbon sheets and PSs refer to plum stones (carbon precursor).

Synthesis of SnO_2 microsphere decorated porous carbon-derived plum stones

In a glass beaker contains 70 mL of DI water, 2 g of PPSs were dispersed and then in the same beaker 5 g of $SnCl_2.2H_2O$ was dissolved followd by magnetic stirring for 1 h. Then, the dispersion was transferred to stainless steel autoclave lined with Teflon vessels of 100 mL capacity. Then heated at 150 °C for 24 h. After cooling to ambient temperature, the obtained composite was washed with DI and menthol, respectively, and then dried at 100 °C under vacuum for 3 h. The developed composite was denoted as PPSs-SnO_2.

Synthesis of PS-PPSs and PS-PPSs-SnO_2 composites

In PS solution dissolved in chloroform different mass ratios of PPSs (10 and 20 mass%) were dispersed individually, then mechanically stirred for 6 h producing new PS composites (Table 1). On the other hand, PPSs-SnO_2 of 10 and 20 mass% were also dispersed in PS solution separately

Table 1 Composition of virgin PS polymer and their composites

Sample code	PS/mass %	PPSs/mass %	PPSs-SnO2/ mass %
PS	100	0	0
PS-PPSs10	90	10	0
PS-PPSs10	80	20	0
PS-PPSs-SnO210	90	0	10
PS-PPSs-SnO220	80	0	20

using the same procedure as mentioned above. Afterward, the solvent was evaporated and samples were compressed and molded separately for 10 min. The blank PS was molded and compressed. The obtained composites denoted as PS-PPSs10 (20) and PS-PPSs-$SnO_2$10 (20) as number refers to mass loadings in mass% of PPSs and PPSs-SnO_2 as shown in Table 1.

Characterization

The structure of developed nanoporous carbon derived from plum stones and decorated with SnO_2 microsphere was studied using Fourier transform infrared spectroscopy (FT-IR). The SEM images of the samples were taken using a scanning electron microscope (QuantaFEG-250, operating at a voltage of 20 kV) equipped with energy-dispersive spectroscopy (EDS). The thermal analysis of the developed composites was evaluated TGA 50 (TA Shimadzu, Inc.) at a temperature range from ambient temperature to 750 °C under inert atmosphere. The textural properties of the developed PPSs were evaluated via N_2 adsorption measurements at regular conditions of measurements (Pressure of 100 kPa and temperature of 77 K) (MicrotracBel, Corp. BELSORP-Max). The sample was degassed at 200 °C for 10 h before N_2 adsorption. The pore size distribution (PSD) was deduced from the desorption branch of the nitrogen isotherm using Barrett–Joyner–Halenda (BJH) method [30]; moreover, the total pore volume was detected from nitrogen adsorbed at P/P0 = 0.99. The flammability properties of the blank and developed PS-based composites were studied using rate of burning via UL94 (horizontal test) based on IEC 60695-11-10 standard [31]. Moreover, the LOI test was implemented for all samples by an oxygen index instrument. Additionally, the antibacterial ability of the developed polymer composite was evaluated against *E-coli* bacteria using AATCC standard test method 147–2004 [32].

Results and discussion

Synthesis approach of sustainable porous flame retardants

The valorization of biomass is appreciated approach from economic and environmental point of view and adhered to the sustainable development goals (SDGs) which strongly recommends the recycling of biomass to valuable materials useful for high-tech applications [33]. Hence, in response to these calls, nanoporous carbon sheets were developed from plum stones (fruit-by-products) using one-pot carbonization step as presented in Fig. 1. Interestingly, the developed porous carbon sheets were converted from PSs as renewable carbon precursor with conversion of 35% yield. In this regard, based on our synthesis procedure (35 % conversion) and annual production of Plum in Egypt (14775 tonnes/ year) and mass of PSs, scalable amount of 517,12 tonnes/year porous carbon sheets can be produced annually. Thus, affords scalable amounts which are suitable for various applications such as flame retardants, gas storage, water treatments and polymer reinforcements. The elemental composition of PPSs stated that PPSs composed of carbon (C), oxygen (O) and nitrogen (N) which played a vital role

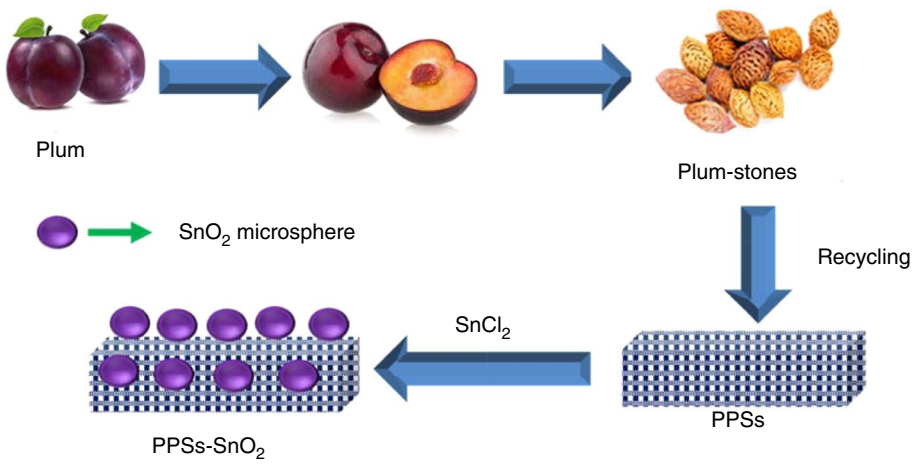

Fig. 1 Schematic representation diagram displaying the green synthesis of renewable porous composite flame retardant

in flame retardancy effect and other traces of metals. This is in addition to high pores covered the PPSs surface (as seen below). Interestingly, SnO_2 microspheres were synthesized on the surface of PPSs via hydrothermal process displaying uniform decoration of SnO_2 microspheres on porous PPSs surface as shown in Fig. 1. The developed composites structure presents new, cost-effective and innovative flame-retardant materials capable of achieving better flame retardancy and antibacterial behavior for thermoplastic polymers as indicated below.

Structural, morphological and textural characterization of developed flame retardants

The structure of PPSs and PPSs-SnO_2 composite was elucidated using FT-IR spectroscopy and XRD. Figure 2a represents the FT-IR spectra of PPSs which reflects the characteristic absorption peaks of porous carbon doped with nitrogen and oxygen species. The absorption peak noticed at 1080 cm^{-1} corresponds to stretching vibration of C–O [24, 34]; however, the absorption peak detected at 1179 cm^{-1} is assigned to C–N stretching vibration (Fig. 2a) [35]. Interestingly, the absorption peak observed at 1582 cm^{-1} is ascribed to stretching vibration of C=C of aromatic skeleton ring of carbon [24, 34, 35]. Moreover, the absorption peak situated at 877 cm^{-1} is assigned to out-of-plane C-H bending (Fig. 2a) [24]. Additionally, the stretching vibration of O–H peak was noticed at 3427 cm^{-1} [24]. For PPSs-SnO_2, in addition to absorption peaks which are characteristic to carbon structure, new absorption peak was noticed at 590 cm^{-1} which is attributed to Sn–O–Sn antisymmetric vibration [36, 37]. This demonstrates that the synthesis of PPSs and PPSs-SnO_2 was successful. On the other hand, the as-developed PPSs and PPSs-SnO_2 were studied using XRD. Figure 2b displays two broad diffraction peaks positioned at ~ 23° and 43° which are correspond to the (002) and (001) diffraction patterns of amorphous graphitic carbons, respectively [38, 39]. However, for PPSs-SnO_2, the diffraction peaks characteristic to SnO_2 (rutile) was observed [40, 41]. Hence, the characteristic diffraction patterns of SnO_2 were noticed at the following positions 26.4° (110), 33.3° (101), 51,77° (211), 64.2° (122) and 78.7° (321) [17, 42], thus confirming the SnO_2 microsphere synthesis on the PPS surface (Fig. 2b). On the other hand, the morphological properties of the PPSs and its developed composite PPSs-SnO_2 were studied using microscopic tools. Figure 3a represents the SEM image of PPSs which displays porous carbon structure contains various surface pores and this clearly obvious at high magnification image (Fig. 3b). Besides, the developed nanoporous carbon was existed in nanoporous carbon sheets morphology as visualized in Fig. S1. For PPs-SnO_2, the SEM image reflects the porous structure of PPSs which is decorated with spherical SnO_2 microsphere of an average diameter of 2 µm (Fig. 3c, d). Moreover, the high magnification SEM image of SnO_2 microsphere displayed that the SnO_2 microsphere surrounded by nanoparticles of an average size of 80–100 nm

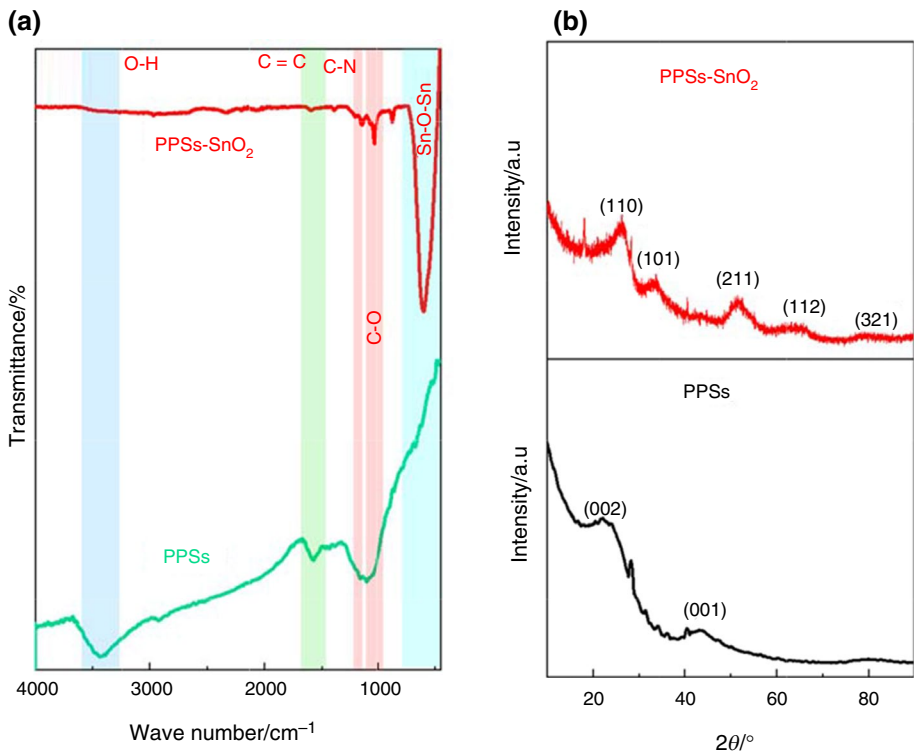

Fig. 2 **a** FT-IR spectra of PPSs and PPSs-SnO_2 and **b** XRD patterns of PPSs and PPSs-SnO_2

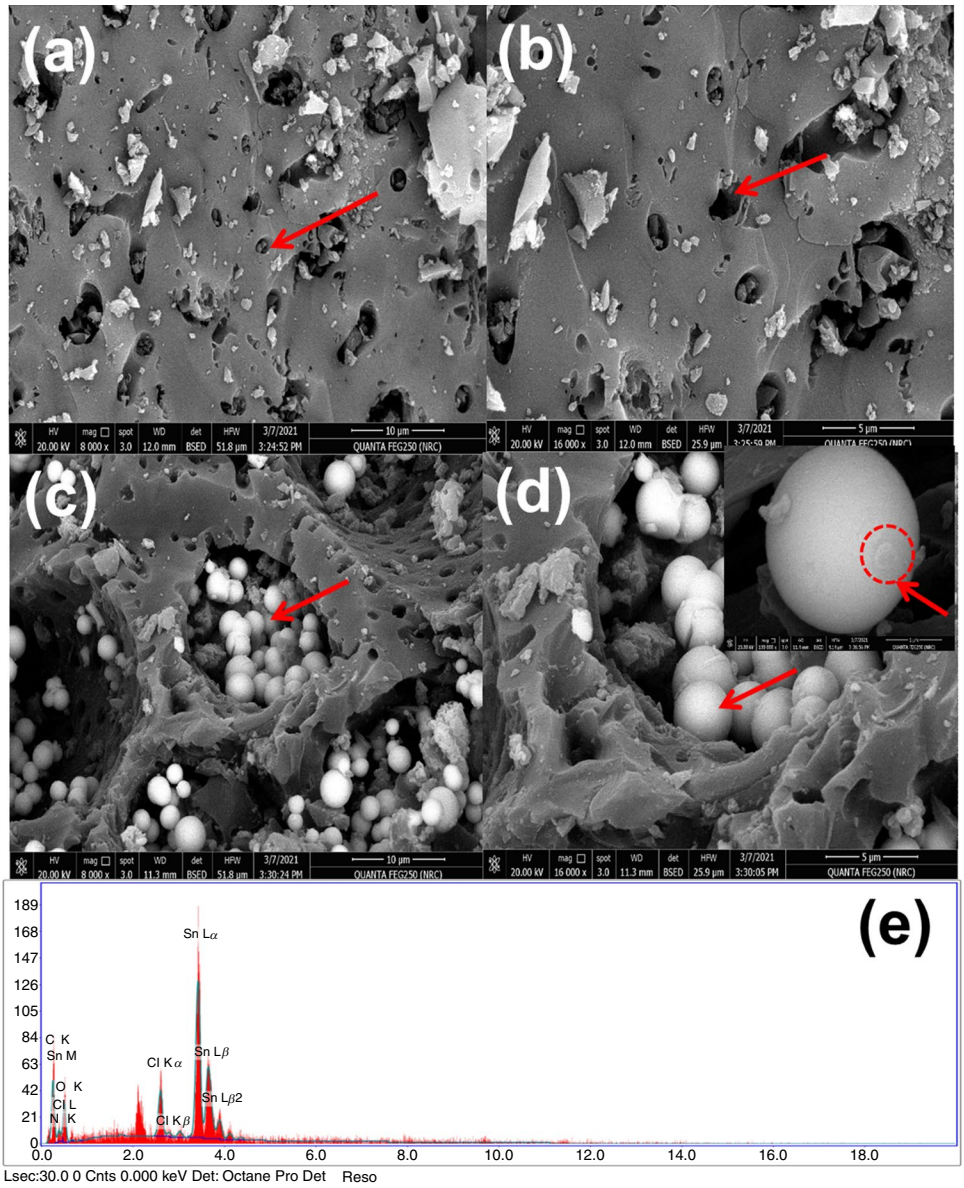

Fig. 3 SEM images of **a** PPSs, **b** PPSs at high magnification, **c** PPSs-SnO_2, **d** PPSs-SnO_2 at high magnification (inset reflects the decorated nanoparticles on SnO_2 microsphere surface) and **e** EDS spectra of PPSs-SnO_2 displaying elemental composition

as shown in Fig. 3d and Fig. S2a and b. Furthermore, the elemental composition of PPSs-SnO_2 was investigated using EDS equipped with SEM. Figure 3e represents the elemental composition which was found to be C (57.31 At. %), O (25.86 At. %), Sn (12.56 At. %), N (0.16 At. %) and Cl (4.09 At. %; which stemmed from unreacted salt). This affirms the existence of SnO_2 microsphere decorated on PPSs surface (Fig. 3e). It is also noted the Sn/C ratio was found to be 0.22 which indicates the ratio was almost 20%.

Additionally, the textural properties of the PPSs were studied using nitrogen sorption process (adsorption–desorption) and the isotherms were conducted at 77 K and 100 kPa. The N_2 isotherms of PPSs displayed type-IV isotherms which is ascribed to mesoporous materials (Fig. 4a) [43]. Also, little hysteresis was noticed (Fig. 4a). The specific surface area (SSA-BET) was found to be 165 $m^2\ g^{-1}$; however, the total pore volume (TPV) was detected to be 0.085 $cm^3\ g^{-1}$ (Fig. 4b). The developed porosity of PPSs was elucidated by the existence of mesopores of an average size of 2.1 nm (Fig. 4b). As shown below, the formed mesopores on the surface of PPSs played a vital role in the flame retardancy action because it is desirable for the capture of combustible gases to slow down the heat and mass transfer and also trap the emitted toxic gases.

Thermal stability and morphological properties of developed polymer composites

The thermal behavior of the blank PS and their developed composites were studied using thermogravimetric analysis from ambient temperature to 750 °C. The thermograph of virgin PS shows only one main decomposition step initiated (onset decomposition temperature) at ~ 350 °C giving rise zero char residue. After incorporation of 10 mass% of PPSs to PS matrix, the curve of PS-PPSs10 reflects similar thermal behavior with main decomposition step as indicated in Fig. 5b, in addition to small mass loss below 100 °C which is ascribed to trapped moisture. However, the role of PPSs was reflected in higher char residue formed at 750 °C which was found to be 9.01 mass% (Fig. 5b). This is demonstrating a good flame retardancy trend, and this is could be due to the ability of PPSs for inducing PS chains for forming char layer and absorbing the combustible gases. Interestingly, similar thermal behavior to PS-PPSs was observed when PPSs-$SnO_2$10 was incorporated by 10 mass% in PS composite (PS-PPSs-$SnO_2$10). However, significant char residue was formed recording 11.54 mass% which affirms the catalytic role of SnO_2 microsphere in combustion process of polymer composite facilities protective char layer formation. This encourages PS chains for forming protective char layer rather than complete thermal pyrolysis. Moreover, this is corroborated by triggering PS chains for char formation by 2.54% superior than PPSs alone (SnO_2 free) and reinforced the char layer (Fig. 5c). On the other hand, when the mass loading of PPSs twofold increases (20 mass%) in PS matrix, its tendency for char formation was little decreased recording char residue of 7 mass% for PS-PPSs20 (Fig. 5d). This trend was also noticed in curve of PS-PPSs-$SnO_2$20 (Fig. 5e).

The dispersion of flame-retardant fillers in polymeric matrix played a significant role in flame retardancy performance; hence, uniform dispersion of flame retardant in polymer matrix reproduces better action. Therefore, the dispersion of PPSs-SnO_2 in PS was evaluated using microscopic techniques. Figure 6a represents the SEM image of PS-PPSs-SnO_2 (10 mass% loading) which displays uniform dispersion of PPSs-SnO_2 throughout the PS matrix chains and wrapped with PS chains. This was confirmed at high magnification SEM image which visualizes the well dispersion of PPSs-SnO_2 in PS matrix and wrapped with PS chains

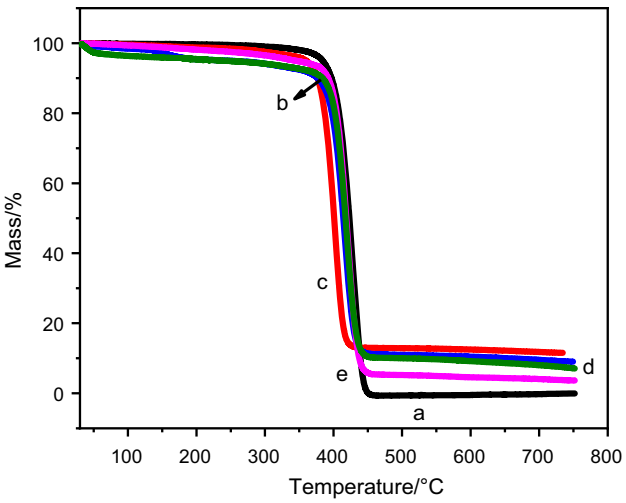

Fig. 5 TGA curves of **a** PS, **b** PS-PPSs10, **c** PS-PPs-$SnO_2$10, **d** PS-PPs20 and **e** PS-PPSs-$SnO_2$20

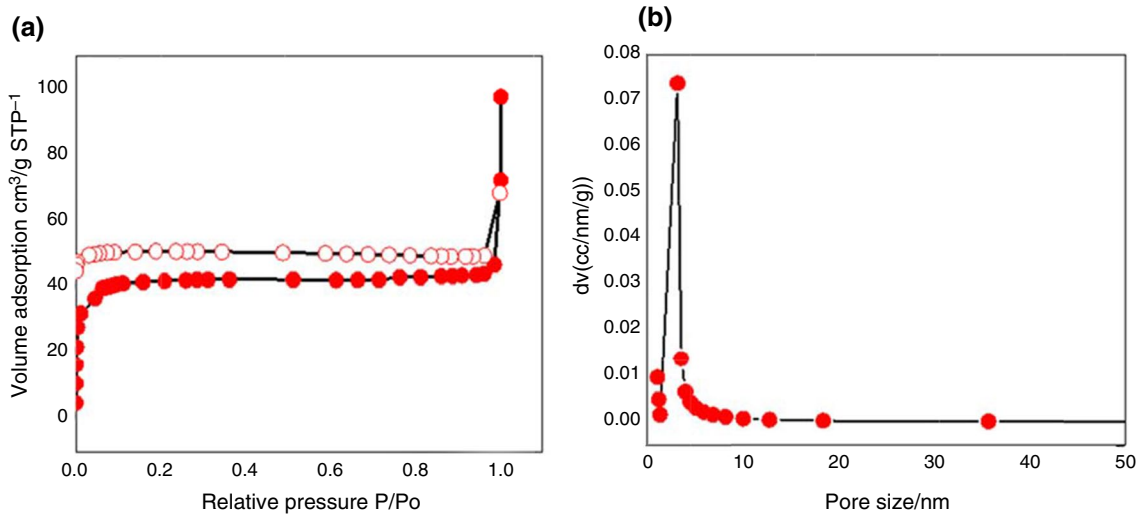

Fig. 4 **a** N_2 adsorption (closed symbol)-desorption (open symbol) isotherms for plum stones derived nanoporous carbon **b** PSDs of plum stones derived nanoporous carbon

(Fig. 6b). Interestingly, the SEM image at further high magnification power clearly indicates that no aggregation was detected and good interfacial adhesion between PPSs-SnO_2 and PS chain was occurred as shown in Fig. 6c.

The Flame retardancy properties of developed polymer composites

The fire hazards of neat PS and their developed PS composites were assessed. Therefore, the flammability properties were studied by measurement of rate of burning (Horizontal test) which implemented using UL94 flame chamber based on IEC 60,695–11-10 [31], this is in addition to limiting oxygen index (LOI) according to ISO standard 4589 [44] and the data are tabulated in Table 2. The blank PS was burned quickly once ignited recording high rate of burning value of 46.5 mm min^{-1}. However, after inclusion and dispersion of PPSs in PS matrix by lower mass loading (10 mass%), the rate of burning was significantly reduced recording 29 mm min^{-1}. Additionally, by dispersing a higher mass loading of PPSs, the flame retardancy behavior was improved and obtaining a rate of burning of 24 mm min^{-1}. This flame retardancy action was attributed to PPSs' capacity to induce PS chains to form a protective char layer separating the melting zone from the flaming one, which in turn retarded mass and heat transmission [2, 9]. In addition to this, PPSs have a rich mesopores structure that allows them to collect combustible gases (the fuel for fire) generated during the pyrolysis of PS chains. This stops the combustion reaction, which extinguishes the flame (Table 2). This was attained in PS-PPSs20 sample which self-extinguish after 55 mm as burnt distance compared to 75 mm for blank and PS-PPSs10 samples. This decrease in fire hazard was supported by a steady increase in LOI value, which showed 22% for PS-PPSs20 as opposed to 18 for PS (Table 2), confirming the usefulness of the protective char layer strength in preventing the inclusion of oxygen to the flame zone. Interestingly, once the PPSs-SnO_2 (lower mass loading (10 mass%) was dispersed in PS matrix the rate of burning of PS-PPSs-$SnO_2$10 was further reduced recording 22 mm min^{-1} compared to 46.5 mm min^{-1} for blank PS (Table 2). The flame retardancy behavior was improved achieving inferior rate of burning of 20.6 via dispersing a higher mass loading of PPSs-$SnO_2$20 in PS (PS-PPSs-$SnO_2$20). This flame retardancy effect of PPSs-SnO_2 was further proved by higher LOI value which achieved 24.5% in PS-PPSs-$SnO_2$10 (Table 2). Thus, superior flame retardancy was attained after decoration of SnO_2 microspheres on the surface of porous PPSs. Then affords a catalytic effect of SnO_2 during polymer composite combustion reaction and

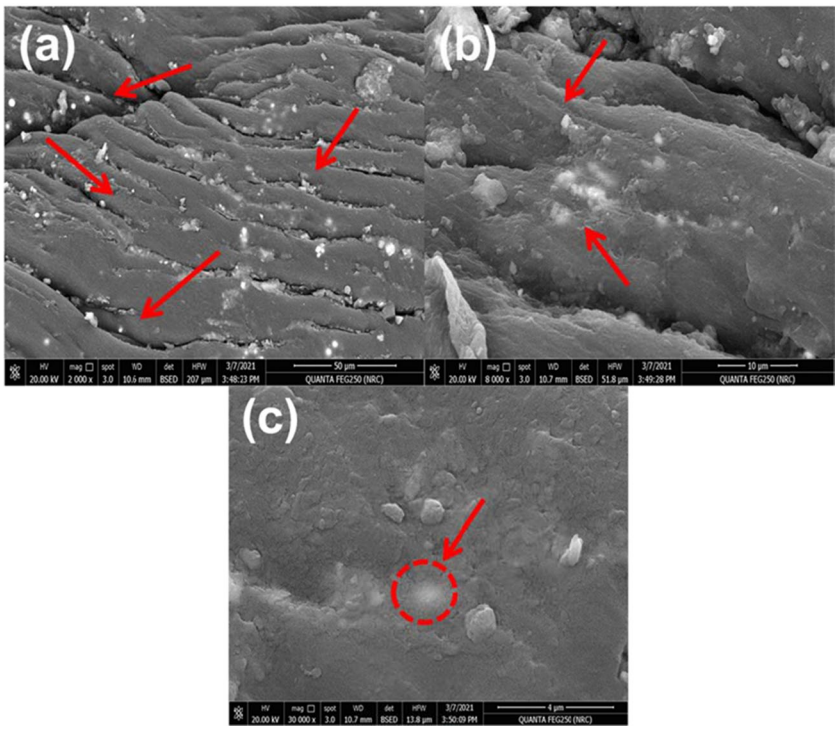

Fig. 6 SEM image of **a** PS-PPSs-$SnO_2$10, **b**, **c** PS-PPSs-$SnO_2$10 at high magnifications displaying the well dispersion in PS matrix

Table 2 Flammability properties of PS and its developed composites

Sample code	[a]Distance/mm	[b]Time/sec	[c]Rate of burning/ mm min^{-1}	[d]Reduction percent/%	LOI/%
PS	75	106	46.5	0	18
PS-PPSs10	75	155	29	37.6	21
PS-PPSs20	55	137	24	48	22
PS-PPSs-$SnO_2$10	70	189	22	52.6	24.5
PS-PPSs-$SnO_2$20	75	218	20.6	56	24

[a]Average distance

[b]Average time

[c]Average rate of burning

[d]Reduction of rate of burning

in turn directs the formation of dense and compact protective char layer rather than decomposition of PS chains. Because of this, the constructed protective barrier was strong enough to separate the PS pyrolysis zone from the burning zone, delay heat and mass transfer and ultimately cause the combustion process to self-extinguish (Fig. S3) [16, 17]. Additionally, porous PPSs induce char formation process and capture of combustible gases inside its porous structure. On the other hand, the flame retardancy action was further elucidated via investigation of char residue after UL94 test (horizontal test). Based on the proposed flame retardancy action, which is summarized as there is a synergistic flame retardancy action between PPSs and SnO_2 microspheres. First, the PS combustion reaction was catalyzed by SnO_2 microspheres, allowing for the quicker creation of a dense, protective char layer that effectively separates the pyrolysis and burning zone. Secondly, in addition to confining the flammable gases in its porous structure and delaying mass and heat transfer, the nitrogen ingredient in PPSs stimulates PS chains to build a protective char layer. Thus, affords self-extinguishing process to the flame as represented in Fig. 7. Additionally, Fig. 8a and b represents the SEM images of char residue formed after combustion of blank PS in UL94 which shows porous and broken char residue and then facilities the escape of combustible gases to flame zone. Thus, affords a fuel for combustion reaction and this was supported from the poor char barrier after burning as shown in Fig. S3. However, the SEM image of char residue after combustion of PS-PPSs-SnO_2 displays compact and dense protective char layer and visualizes the well dispersion of PPSs-SnO_2 which in turn strengthening the protective char layer (Fig. 8c, d). High-magnification SEM images clearly show this phenomenon, which reflects the compactness and density of the reinforced char layer (Fig. 8e). Also, obvious proof was found from digital photos of PS-PPSs-$SnO_2$10 after horizontal test and which corroborates rich and compact char layer formed (Fig. S3).

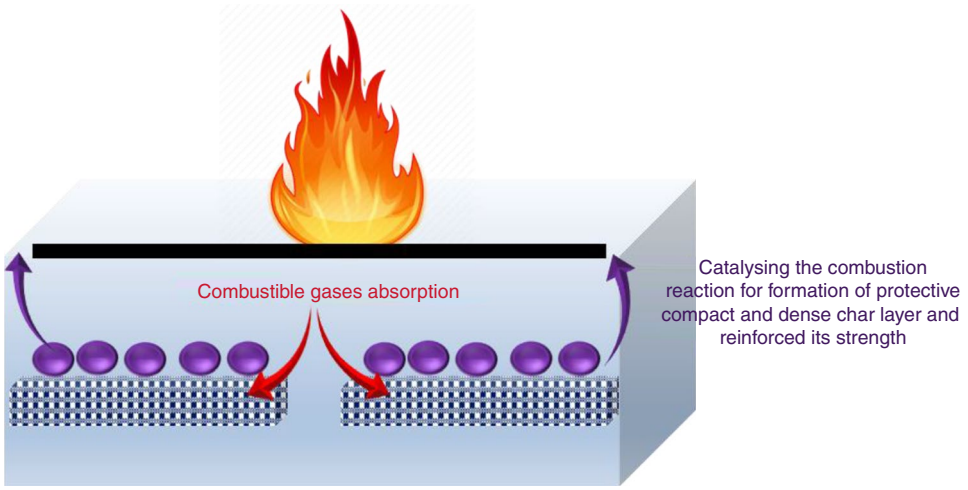

Fig. 7 Schematic diagram representing the flame retardancy mechanistic action of green developed flame retardant for polystyrene composite

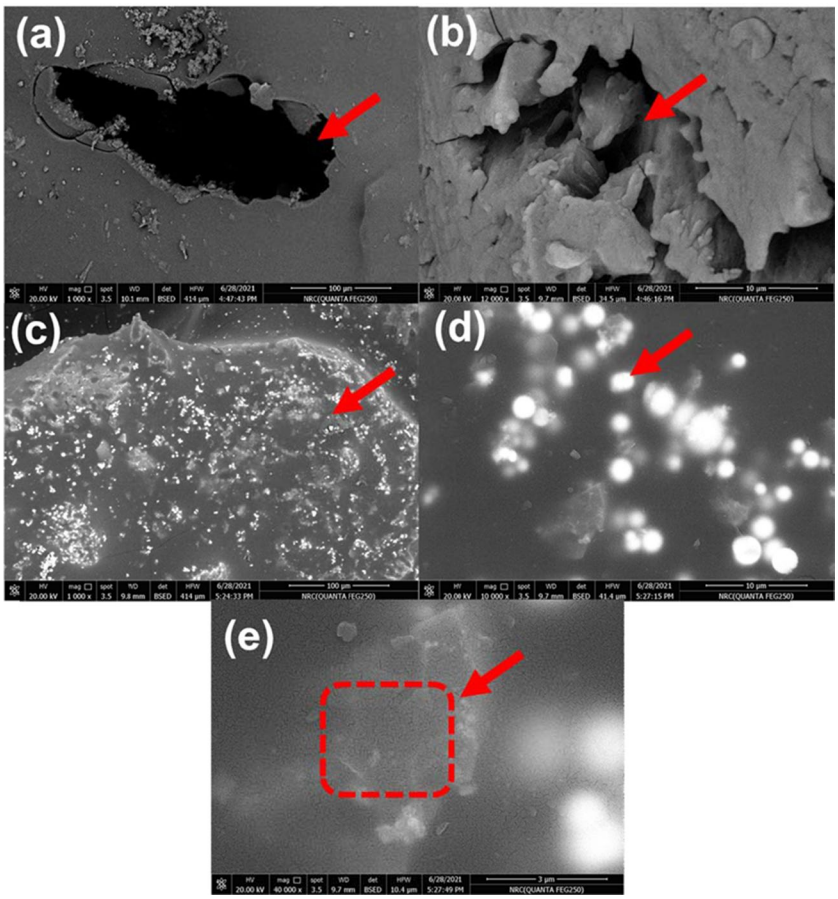

Fig. 8 SEM image of formed char after UL94 test of **a** PS, **b** PS at high magnification, **c** PS-PPSs-$SnO_2$10 and **d**, **e** PS-PPSs-$SnO_2$10 at high magnification

Noteworthy to note that, the porous structure role in flame retardancy mechanism is summarized as stated below in two main routes. The first route; the pores of porous structure trap the released combustible gases which emitted in the beginning of combustion process and upon thermal pyrolysis of polymer chains. Then hinders the flaming process and slowing down the back-heat release and in turn restricts mass and heat transfer and in turn provide flame retardation process (Figs.7, 8). Secondly, porous structure can easily accommodate and store the released toxic gases during combustion process such as CO, CO_2 and smoke which suppress the emission of these toxic gases and their harmful effect and this conclusion is consistent with our previous study [9].

The antibacterial properties of developed polymer composites

The capability of polymer composites for inhibiting the growth of bacteria on their surface is strongly required nowadays and is considered as a smart merit for the thermoplastic polymer composites. Hence, the ability of PPSs-SnO_2 for inhibiting the growth of *Escherichia coli* bacteria (gram-negative bacteria) was evaluated. It was found that PS composites contained PPSs-SnO_2 has strong ability to inhibit the growth of bacteria compared to PS composite free of SnO_2 microspheres. The developed composite achieved positive antibacterial behavior recording clear inhibition zone of 11 mm for PS-PPSs-$SnO_2$10 compared to zero clear inhibition zone for PS-PPSs10. This positive antibacterial activity was ascribed to the role of SnO_2 for inhibiting the growth of *Escherichia coli* bacteria [44] as shown in Fig. 9. Thus, this system provides good flame retardant performance superior than reported [45, 46].

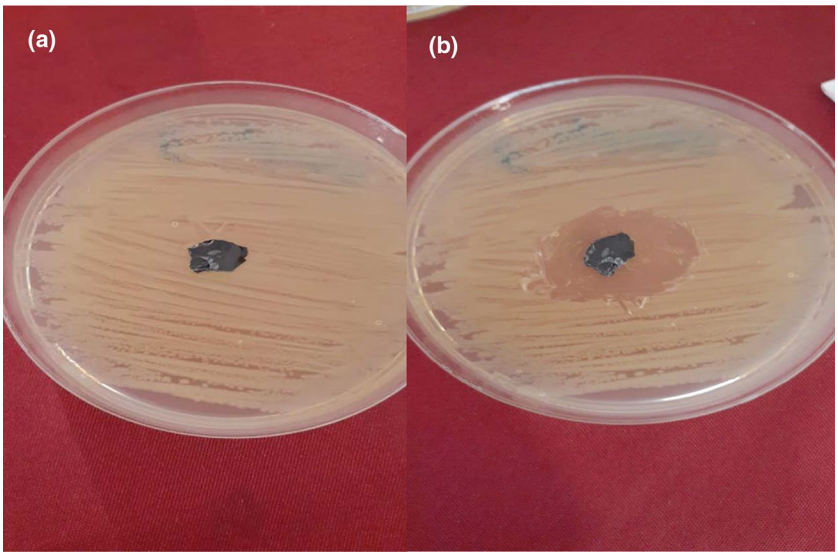

Fig. 9 Digital photos of clear bacterial inhibition zone for **a** PS-PPSs10 and **b** PS-PPSs-$SnO_2$10

Conclusions

Sustainable porous carbon sheets and their composites with SnO_2 microspheres were developed and exploited as an efficient and green flame retardant for thermoplastic polymers. By using a single recycling carbonization procedure, plum stones, a fruit-by-product, were converted to mesoporous carbon, achieving one of the sustainable development goals. The developed porous carbon is characterized by mesopores with an average pore size of 2.1 nm and specific surface area of 165 $m^2\ g^{-1}$; this is in addition to naturally doped nitrogen species. Afterward, SnO_2 microspheres of an average size of 2 µm were grown on the surface of porous carbon in uniform dispersion regime. The new porous carbons and their composites based on SnO_2 microspheres were dispersed individually in polystyrene yielding different polymer composites. The flame retardancy of the new polymer composites was strongly enhanced achieving reduction in rate of burning by 56% compared to blank sample and improving LOI by 36%. This superior fire safety was stemmed from the synergistic effect between charring and combustible gases absorption tendency of porous carbon contained nitrogen, and catalytic effect of SnO_2 microsphere which afford compact and dense protective char barrier retard mass and heat transfer. Moreover, the developed composite affords antibacterial behavior recording clear inhibition zone of 11 mm compared to zero for blank sample.

Supplementary Information The online version contains supplementary material available at https://doi.org/10.1007/s10973-023-12066-8.

Funding Open access funding provided by The Science, Technology & Innovation Funding Authority (STDF) in cooperation with The Egyptian Knowledge Bank (EKB).

References

1. Zhu S-E, Yang W-J, Zhou Y, Pan W-H, Wei C-X, Yuen ACY, Chen TBY, Yeoh GY, Lu HD, Yang W. Synthesis of zinc porphyrin complex for improving mechanical, UV-resistance, thermal stability and fire safety properties of polystyrene. Chem Eng J. 2022;442: 136367.
2. Attia NF, Abdel Eal NS, Hassan MA. Facile synthesis of graphene sheets decorated nanoparticles and flammability of their polymer nanocomposites. Polym Degrad Stab. 2016;126:65–79.
3. Guan F-L, Gui C-X, Zhang H-B, Jiang Z-G, Jiang Y, Yu Z-Z. Enhanced thermal conductivity and satisfactory flame retardancy of epoxy/alumina composites by combination with graphene nanoplatelets and magnesium hydroxide. Compos Part B Eng. 2016;98:134–40.
4. Pan Y-T, Wang X, Li Z, Wang D-Y. A facile approach towards large-scale synthesis of hierarchically nanoporous SnO_2@Fe_2O_3 0D/1D hybrid and its effect on flammability, thermal stability and mechanical property of flexible poly(vinyl chloride). Compos B. 2017;110:46–55.
5. Shi Y, Liu C, Fu L, Yang F, Lv Y, Yu B. Hierarchical assembly of polystyrene/graphitic carbon nitride/reduced graphene oxide nanocomposites toward high fire safety. Compos Part B. 2019;179: 107541.
6. Attia NF, Zayed Z. Nanoparticles decorated on resin particles and their flame retardancy behavior for polymer composites. J Nanomater. 2017;2017:1–8.

7. Si JY, Tawiah B, Sun WL, Lin B, Wang C, Yuen ACY, Yu B, Li A, Yang W, Lu HD, Chan QN, Yeoh GH. Functionalization of MXene nanosheets for polystyrene towards high thermal stability and flame-retardant properties. Polymers (Basel). 2019;11:976.
8. Bao C, Song L, Wilkie CA, Yuan B, Guo Y, Hu Y, Gong X. Graphite oxide, graphene, and metal-loaded graphene for fire safety applications of polystyrene. J Mater Chem. 2012;22:16399–406.
9. Attia NF. Sustainable and efficient flame retardant materials for achieving high fire safety for polystyrene composites. J Therm Anal Calorim. 2022;147:5733–42.
10. Cai T, Wang J, Zhang C, Cao M, Jiang S, Wang X, Wang B, Hu W, Hu Y. Halogen and halogen-free flame retarded biologically-based polyamide with markedly suppressed smoke and toxic gases releases. Compos Part B Eng. 2020;184: 107737.
11. Grause G, Karakita D, Ishibashi J, Kameda T, Bhaskar T, Yoshioka T. Impact of brominated flame retardants on the thermal degradation of high-impact polystyrene. Polym Degrad Stab. 2013;98:306–15.
12. Zhu Z-M, Rao W-H, Kang AH, Liao W, Wang Y-Z. Highly effective flame retarded polystyrene by synergistic effects between expandable graphite and aluminum hypophosphite. Polym Degrad Stab. 2018;154:1–9.
13. Xu Z, Xing W, Hou Y, Zou B, Han L, Hu W, Hu Y. The combustion and pyrolysis process of flame-retardant polystyrene/cobalt-based metal organic frameworks (MOF) nanocomposite. Combust Flame. 2021;226:108–16.
14. Qu H, Wu W, Zheng Y, Xie J, Xu J. Synergistic effects of inorganic tin compounds and Sb_2O_3 on theral properties and flame retardancy of flexible poly (vinyl chloride). Fire Saf J. 2011;46:462–7.
15. Qu H, Wu W, Xie J, Xu J. A novel intumescent flame retardant and smoke suppression system for flexible PVC. Polym Adv Technol. 2011;22:1174–81.
16. He S, Wu W, Zhang M, Han H, Jiao Y, Qu H, Xu J. Reduction in smoke emitted and fire hazard presented by flexible poly (vinyl chloride) through novel synthesis of SnO_2 supported by activated carbon spheres. Polym Adv Technol. 2018;29:2505–14.
17. Hu W, Wu J, Jiao Y, Xie J, Chen J, Xu J. Synthesis of hollow tin dioxide and its improvement of flame retardancy and toughness on poly (vinyl chloride). J Fire Sci. 2019;37:67–80.
18. Meng W, Wu W, Zhang W, Cheng L, Jiao Y, Hongqiang QuH, Xu J. Biotemplated facile synthesis of three-dimensional micro/nanoporous tin oxide:improving the flammable and mechanical properties of flexible PVC. Micro Nano Lett. 2019;14:828–30.
19. Liu F-Y, Zhou X-L, Zhao H, Hu W-D, Xu J-Z, Jiao Y-H, Hong-Qiang Qu H-Q. The synergistic flame retardant, smoke suppressant, and thermal degradation properties of spherical $CoSn(OH)_6$ and ammonium polyphosphate on epoxy resin. J Therm Anal Calorim. 2022. https://doi.org/10.1007/s10973-021-11188-1.
20. Liu T, Wang Z, Sun Y. Manipulating the morphology of nanoscale zero-valent iron on pumice for removal of heavy metals from wastewater. Chem Eng J. 2015;263:55–61.
21. Pan Y-T, Trempont C, Wang D-Y. Hierarchical nanoporous silica doped with tin as novel multifunctional hybrid material to flexible poly(vinyl chloride) with greatly improved flame retardancy and mechanical properties. Chem Eng J. 2016;295:451–60.
22. Pan Y-T, Castillo-Rodríguez M, Wang D-Y. Mesoporous metal oxide/pyrophosphate hybrid originated from reutilization of water treatment resin as a novel fire hazard suppressant. Mater Chem Phys. 2018;203:49–57.
23. Attia NF. Organic nanoparticles as promising flame retardant materials for thermoplastic polymers. J Therm Anal Calorm. 2017;127:2273.
24. Park J, Jung M, Jang H, Lee K, Attia NF, Oh H. A facile synthesis tool of nanoporous carbon for promising H_2, CO_2, and CH_4 sorption capacity and selective gas separation. J Mater Chem A. 2018;6:23087.
25. Attia NF, Park J, Oh H. Facile tool for green synthesis of graphene sheets and their smart freestanding UV protective film. Appl Surf Sci. 2018;458:425–30.
26. Jung M, Park J, Lee K, Attia NF, Oh H. Effective synthesis route of renewable nanoporous carbon adsorbent for high energy gas storage and CO_2/N_2 selectivity. Renew Energy. 2020;161:30–42.
27. https://www.atlasbig.com/en-gb/countries-by-plum-production. Accessed 07 July 2022.
28. Attia NF, Elashery SEA, Zakria AM, Eltaweil AS, Oh H. Recent advances in graphene sheets as new generation of flame retardant materials. Mater Sci Eng B. 2021;274:115460.
29. Attia NF, Hegazi EM, Abdelmageed AA. Smart modification of inorganic fibers and flammability mechanical and radiation shielding properties of their rubber composites. J Therm Anal Calorim. 2018;132:1567–78.
30. Barrett EP, Joyner LS, Halenda PP. The determination of pore volume and area distributions in porous substances. I. Computations from nitrogen isotherms. J Am Chem Soc. 1951;73:373–80.
31. International standard IEC 60695-11-10, fire hazard testing part 11–10: test flames-50 W horizontal and vertical flame test methods.
32. AATCC Test Method (147). Antibacterial activity assessment of textile materials parallel streak methods: parallel streak method, 2004
33. United Nations transforming our world: The 2030 agenda for sustainable development. Available online: https://sdgs.un.org/2030agenda. Accessed on 7 July 2022
34. Peng WC, Chen Y, Li XY. MoS_2/reduced graphene oxide hybrid with CdS nanoparticles as a visible light-driven photocatalyst for the reduction of 4-nitrophenol. J Hazard Mater. 2016;309:173–9.
35. Sevilla M, Valle-Vigón P, Fuertes AB. N-doped polypyrrole-based porous carbons for CO_2 capture. Adv Funct Mater. 2011;21:2781–7.
36. Du Z, Yin X, Zhang M, Hao Q, Wang Y, Wang T. In situ synthesis of SnO_2/graphene nanocomposite and their application as anode material for lithium ion battery. Mater Lett. 2010;64:2076–9.
37. Liu L, An M, Yang P, Zhang J. Superior cycle performance and high reversible capacity of SnO_2/graphene composite as an anode material for lithium-ion batteries. Sci Rep. 2015;5:9055.
38. Zhang JR, Wang X, Qi GC, Li BH, Song ZH, Jiang HB, Zhang XH, Qiao JL. A novel N-doped porous carbon microsphere composed of hollow carbon nanospheres. Carbon. 2016;96:864–70.
39. Cheng P, Li T, Yu H, Zhi L, Liu ZH, Lei ZB. Biomass-derived carbon fiber aerogel as a binder-free electrode for high-rate supercapacitors. J Phys Chem C. 2016;120:2079–86.
40. Cheng M, Hwang C, Pan C, Cheng J, Ye Y, RickJ F, Hwang B-J. Facile synthesis of SnO_2-embedded carbon nanomaterials via glucose-mediated oxidation of Sn particles. J Mater Chem. 2011;21:10705–10.
41. Wang J, Wu W, Wang W, Bao M. Expeditious synthesis of SnO_2 nanoparticles through controlled hydrolysis and condensation of Tin alkoxide in reverse microemulsion. Ceram Int. 2017;43:4702–5.
42. Mali SS, Shim CS, Kim H, Lee MC, Patil SD, Patil PS, Hong CH. Hierarchical SnO_2 microspheres prepared by hydrothermal process for efficient improvement of dye-sensitized solar cell properties. J Nanopart Res. 2015;17:496.
43. Sing KSW, Everett DH, Haul RAW, Moscou L, Pierotti RA, Rouquerol J, Siemieniewska T. Reporting physisorption data for gas/solid systems with special reference to the determination of surface area and porosity (recommendations 1984). Pure Appl Chem. 1985;57:603–19.

44. Amininezhad SM, Rezvani A, Amouheidari M, Amininejad SM, Rakhshani S. The antibacterial activity of SnO_2 nanoparticles against *Escherichia coli* and *Staphylococcus aureus*. Zahedan J Res Med Sci. 2015;17:1053.
45. Attia NF, Saleh BK. Novel synthesis of renewable and green flame-retardant, antibacterial and reinforcement material for styrene–butadiene rubber nanocomposites. J Therm Anal Calorim. 2020;139:1817–27.
46. Attia NF, Afifi HA, Hassan MA. Synergistic study of carbon nanotubes, rice husk ash and flame retardant materials on the flammability of polystyrene nanocomposites. Mater Today Proc. 2015;2:3998–4005.